Experimental Evaluation of the Properties of Veriflex® Shape Memory Polymer

Ing. Jan Klesa

Abstrakt

Polymery s tvarovou pamětí jsou materiály s obrovským potenciálem pro budoucí aplikace. Při ohřevu nad transformační teplotu (dle typu polymeru to může být buď teplota skelného přechodu nebo teplota tání polymeru) dochází k výrazné změně vlastností materiálu. Materiál Veriflex® byl vybrán, protože je dostupný na trhu a má vlastnosti podobné epoxidovým pryskyřicím. Byla provedena analýza DMA (Dynamic Mechanical Analysis) pro určení teploty skelného přechodu v závislosti na frekvenci harmonického cyklického zatěžování a pro vyhodnocení změny elastických vlastností v závislosti na teplotě. Dále byly provedeny tahové zkoušky za normální a zvýšené teploty a byla provedena experimentální simulace pracovního cyklu polymeru s tvarovou pamětí.

Abstract

Shape memory polymers (SMPs) are materials with a great potential for future use. When heated above the transformation temperature they undergo great changes of the mechanical properties. Veriflex® was chosen because of its easy accessibility. Furthermore its properties are similar to epoxy resins which make it very suitable for usage in a wide variety of technical applications. Dynamic mechanical analysis (DMA) was used to determine evolution of the viscoelastic properties versus temperature and frequency under cyclic harmonic loading for evaluation of changes of the elastical properties on temperature. Tensile tests at normal and high temperature were done and working cycle of SMP with 100% elongation was also experimentally simulated.

Klíčová slova

polymery s tvarovou pamětí, analýza DMA, superpozice teplota-frekvence, teorie WLF.

Keywords

shape memory polymers, DMA analysis, temperature-frequency superposition, WLF theory.

1. Introduction

Shape memory polymers are materials which provide huge potential for future applications in many branches. They can be easily applied to morphing structures. They are relatively cheap (compared with other systems used for morphing applications like piezoceramic actuators). Veriflex® shape memory polymer was chosen for this test because of it is accessible on the market and can be easily used for composite material fabrication. When heated from cold state (below the transformation temperature, which can either be the glass transition temperature or the melting temperature of the polymer) to hot state (above the transformation temperature) they undergo transformation which induces great changes of the mechanical properties and some shape memory phenomenon can be observed. The scope was evaluated the properties for future practical applications.

2. DMA Tests

2.1 DMA Testing Facility Description

Dynamic mechanical analysis (DMA) of Veriflex® was done using BOSE Electro Force® equipment. Dependence of storage modulus E', loss modulus E'' and tan δ on temperature and frequency of cyclic harmonic loading was measured. The specimen used for DMA experiments were rectangular with dimensions 5*5*80 mm (see fig. 3). Three specimen were tested, measurements are called multifrequency 1, multifrequency 2 and multifrequency 3. Low stiffness of the specimen at higher temperatures caused problems with sliding (see fig. 2).

Fig. 1. *DMA (Dynamic Mechanical Analyzer) – general view.*

Fig. 2. *Veriflex® specimen after DMA test – sliding of the specimen caused by low stiffness at high temperatures was observed.*

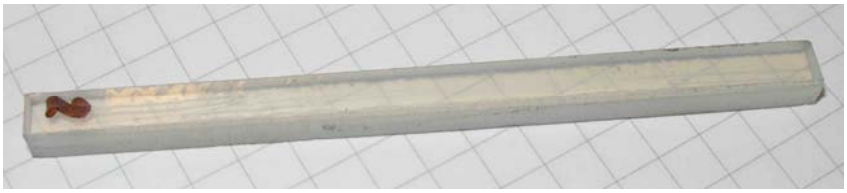

Fig. 3. *DMA test specimen.*

2.2 Dependence of Elastic Properties of Veriflex® on the Temperature

Dependence of storage modulus E', loss modulus E" and tangents delta on temperature for frequencies 0.01, 0.1, 1 and 10 Hz can be seen in fig. 4 to 7. Huge decrease of storage modulus with temperature increase can be seen in fig. 5 (from approx. 1000 MPa at 25° C to

approx. 1 MPa at 90° C. Cole - Cole diagram (dependence of E" on E') is shown in fig. 8. It has only one peak which means that only one transformation occurs at this temperature range.

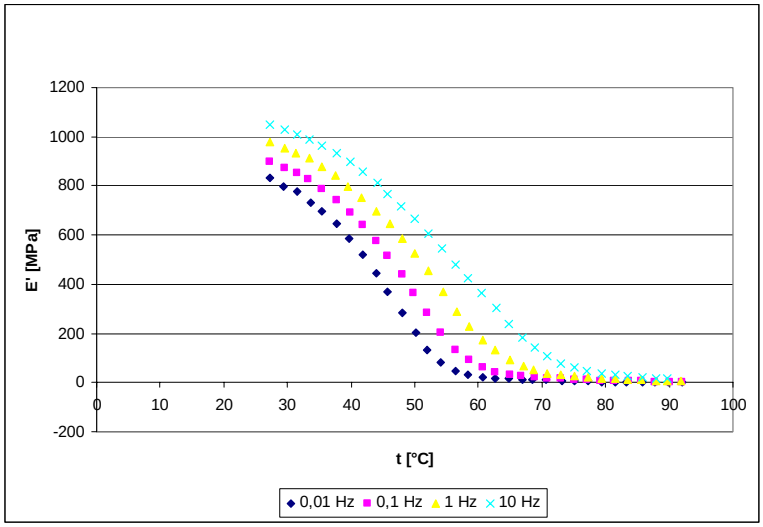

Fig. 4. *Dependence of the storage modulus E' on the temperature (linear scale).*

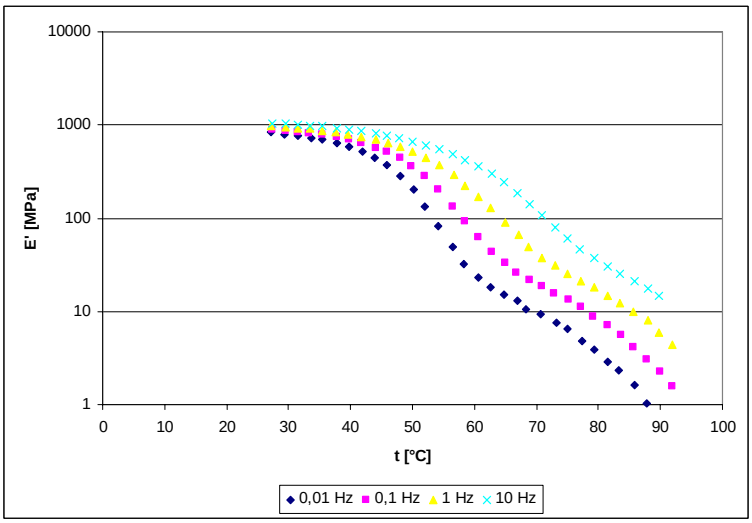

Fig. 5. *Dependence of the storage modulus E' on the temperature (logarithmic scale).*

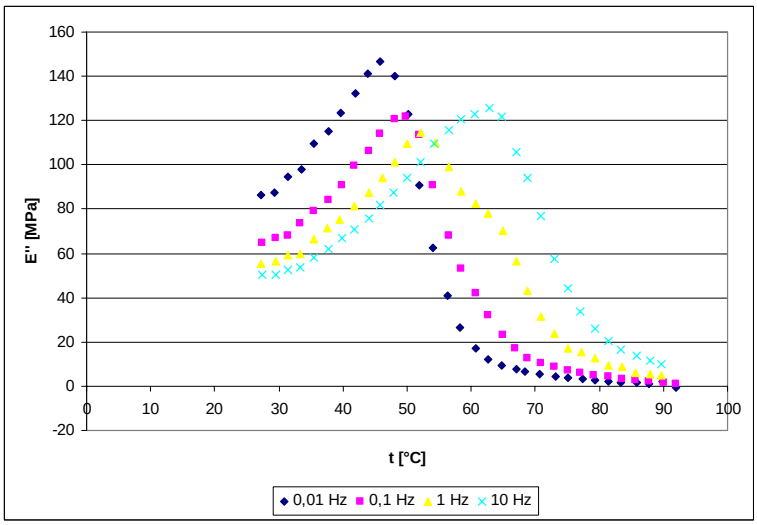

Fig. 6. *Dependence of the loss modulus E'' on the temperature.*

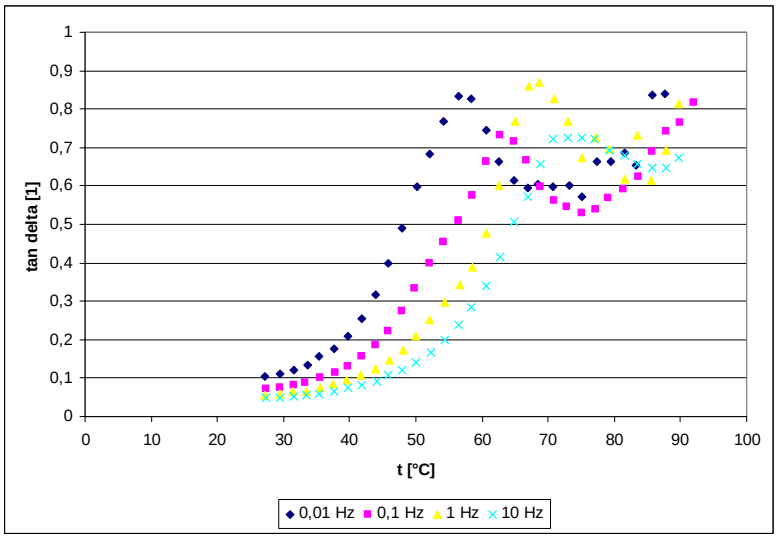

Fig. 7. *Dependence of tangent delta on the temperature.*

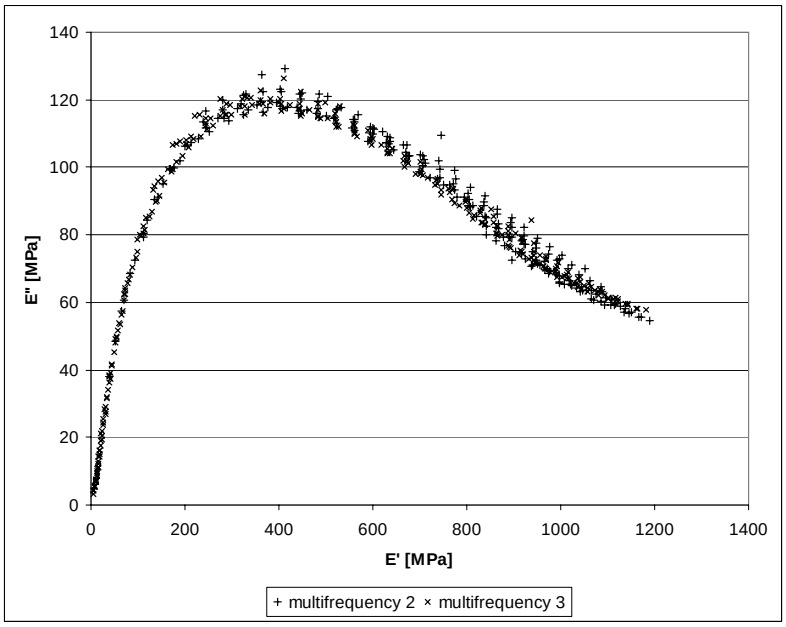

Fig. 8. *Cole – Cole diagram of Veriflex®.*

2.3 Glass Transition Temperature

Glass transition temperature was determined like the peak of loss modulus E'' and the peak of *tan δ*. Each dependency was approximated with cubic polynomial (see fig. 9). The peak was determined like the maximum of this polynomial. The values of the glass transition temperature are shown in fig. 10 and in table 1. When compared with the values of the glass transition temperature in Veriflex® datasheet (i.e. 62° C without any specification), measured values are lower for lower frequencies.

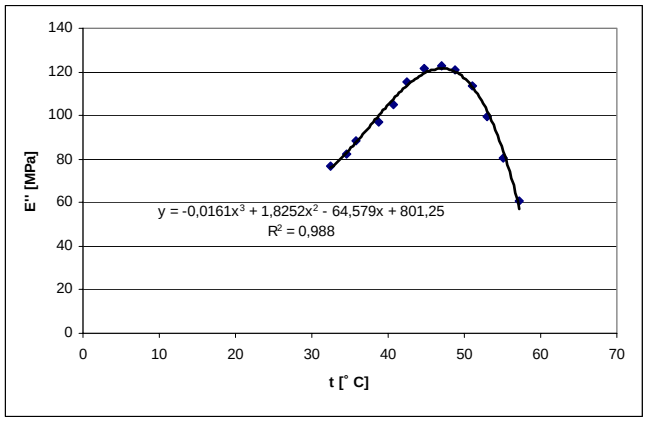

Fig. 9. *Cubic approximation of the loss modulus for finding the peak (for determining of the glass transition temperature).*

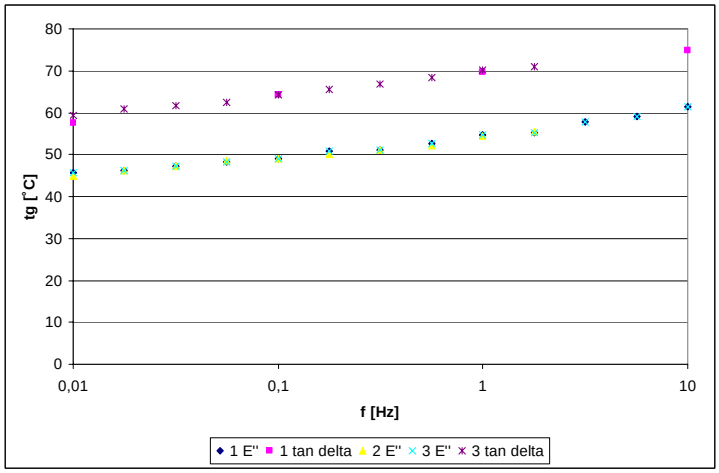

Fig. 10. *Dependence of the glass transition temperature on the frequency of the loading (glass transition temperature was determined as a peak of the loss modulus E'' and at the same time as a peak of tan delta).*

Table 1. *– Dependence of the glass transition temperature on the frequency of cyclic harmonic loading.*

f	multifrequency 1		multifrequency 2		multifrequency 3	
	peak E''	peak tan delta	peak E''	peak tan delta	peak E''	peak tan delta
[Hz]	[° C]	[° C]	[° C]	[° C]	[° C]	[° C]
0,01	45,86	57,55	44,8		45,69	59,45
0,0178			46,25		46,11	60,91
0,0316			47,33		47,23	61,6
0,0562			48,44		48,3	62,41
0,1	48,79	64,33	49,16		49,05	64,26
0,178			49,98		50,76	65,49
0,316			51,01		51,1	66,76
0,562			52,07		52,74	68,31
1	52,35	69,65	54,51		54,76	70,15
1,78			55,39		55,18	70,96
3,16					57,87	
5,62					59,01	
10	61,41	74,88			61,33	

2.4 Master curve for Veriflex®

From the dependencies of storage modulus E', loss modulus E'' and tan delta (see fig. 11) were created master curves for these properties (see fig. 12 to 15). Reference temperature was 45° C. The curve for his temperature is stable and the other curves are let slide horizontally to form master curve. Dependence of horizontal shift factor *a* on temperature was approximated by WLF theory. According to this theory the approximation of a can be written in the form (1).

$$\log a = \frac{-C_1 \cdot (T - T_{ref})}{C_2 + T - T_{ref}} \qquad (1)$$

Universal constants in this formula have following values:

$C_1 = 18.30$
$C_2 = 70.54\ K$

Approximation can be seen in fig. 16. This was done for two measurements called multifrequency 2 and multifrequency 3. The master curves of these measurements are compared in fig. 13 to 15.

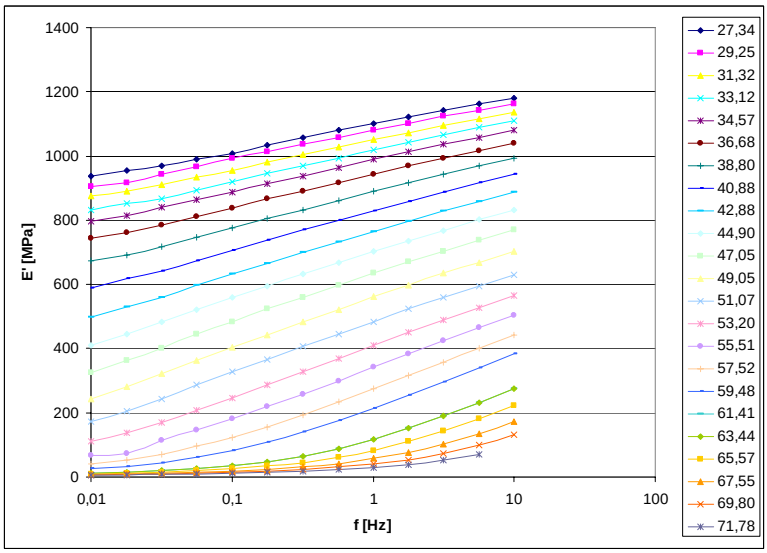

Fig. 11. *Dependence of the storage modulus E' on frequency for different temperatures (measurement multifrequency 3, zero horizontal shift).*

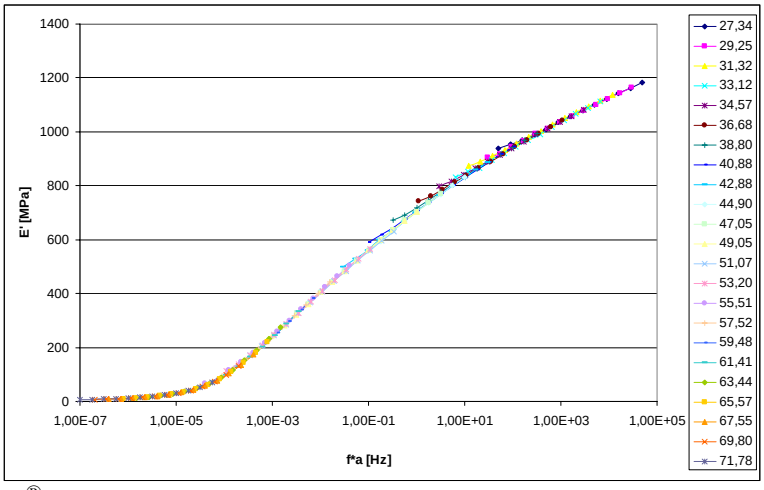

Fig. 12. *Veriflex® master curve for storage modulus E' (measurement multifrequency 3).*

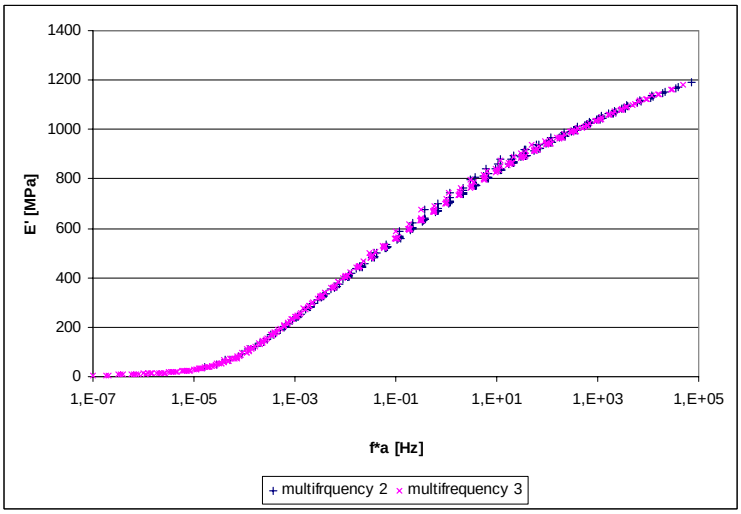

Fig. 13. *Comparison of Veriflex® master curves for storage modulus E' – measurements multifrequency 2 and multifrequency 3.*

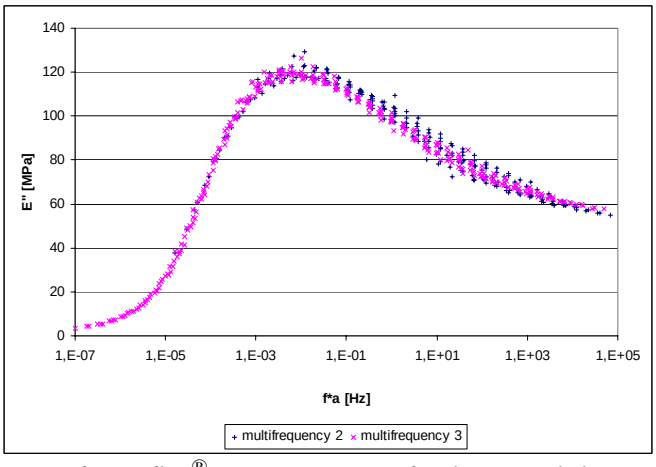

Fig. 14. *Comparison of Veriflex® master curves for loss modulus E'' – measurements multifrequency 2 and multifrequency 3.*

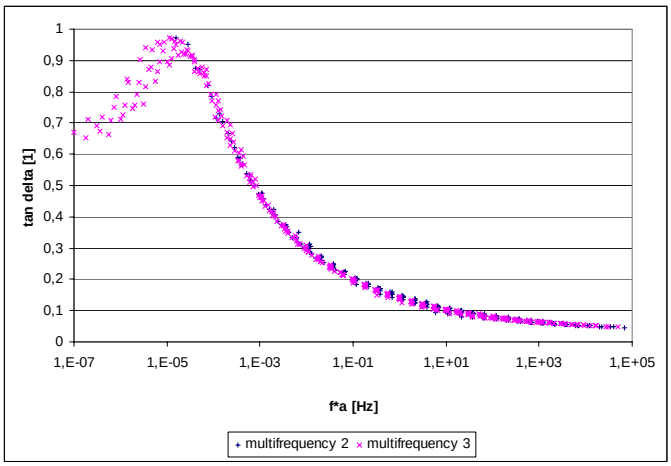

Fig. 15. *Comparison of Veriflex® master curves for tan delta – measurements multifrequency 2 and multifrequency 3.*

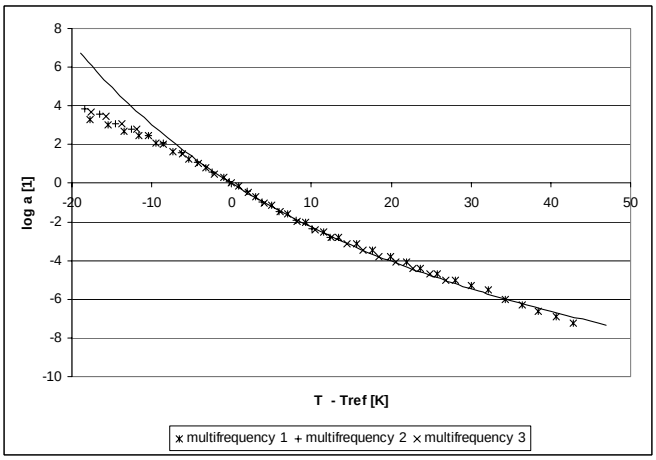

Fig. 16. *Approximation of dependence of horizontal shift factor a on temperature by WLF formula, T_{ref} = 45° C, universal constants: C_1 = 18.30, C_2 = 70.54 K.*

3. Tensile Test

3.1 Tensile Test at 25º C

Tensile test at ambient temperature was done with Veriflex specimen. The cross section of the specimen had dimensions 5*15 mm. Recorded dependence of stress on deformation can be seen in fig. 17. It can be seen that the polymer is quite rigid and fragile at this temperature. Tensile strength σ_{max} of Veriflex® measured during this test is 19.40 MPa (value 22.97 MPa can be found in Veriflex® datasheet). The specimen can be seen in fig. 18, detail of rupture can be seen in fig. 19. The colour of the material changed from clear to white in the zone near to the rupture.

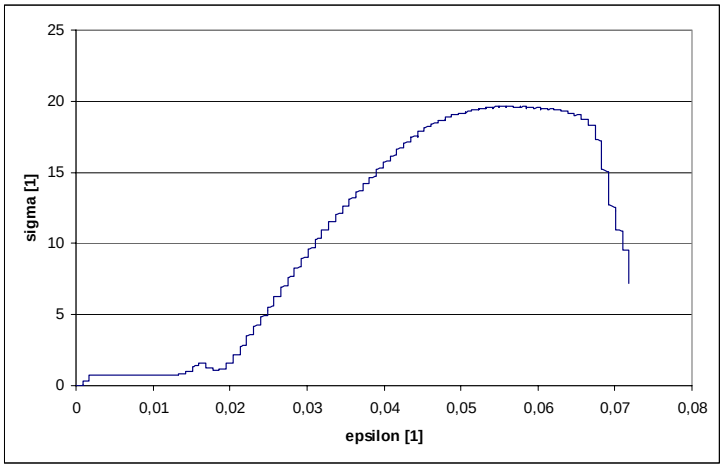

Fig. 17. *Dependence of deformation on stress of Veriflex® shape memory polymer specimen during tensile test at 25° C.*

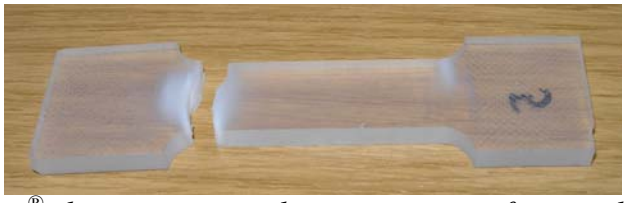

Fig. 18. *Veriflex® shape memory polymer specimen after tensile test at 25° C.*

Fig. 19. *Detail of the rupture of Veriflex® shape memory polymer specimen, tensile test at 25° C.*

3.1 Tensile Test at 70º C

Tensile test at 70º C was done to show different behaviour of the material at higher temperatures. Recorded dependence of stress on deformation can be seen in fig. 20. It can be seen that material is much less stiff. The test was not finished by rupture but she specimen slided. Maximum elongation achieved was approximately 250%. Comparison of the specimen after the test and unused specimen can be seen in fig. 21.

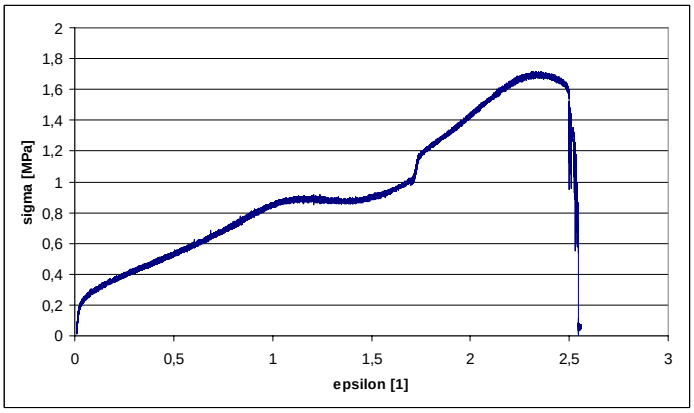

Fig. 20. *Dependence of deformation on stress of Veriflex® shape memory polymer specimen during tensile test at 70° C, the test didn't end with rupture because of sliding of the specimen.*

Fig. 21. *Comparison of Veriflex® specimen – the upper after tensile test at 70° C, the lower was never used for tests.*

4. Working Cycle of Shape Memory Polymer

4.1 Introduction

Working cycle of shape memory polymer is shown in fig. 22. It consists of following parts:

1 permanent shape, polymer is heated above transformation temperature, no deformation and no force is applied
1 – 2 deformation from permanent shape 1 to temporary shape 2 at high temperature (= temperature higher that transformation temperature of the polymer)
2 – 3 relaxation
3 – 4 cooling at constant applied force
4 – 5 applied force is lowered to zero
5 – 6 heating with zero force applied, polymer returns to its permanent shape

Point 6 is close to point 1. Residual deformation can be observed, but it is small compared with deformation in the point 2, which is approximately 100% (depends on the polymer, according to the Veriflex® datasheet maximal deformation is about 200%).

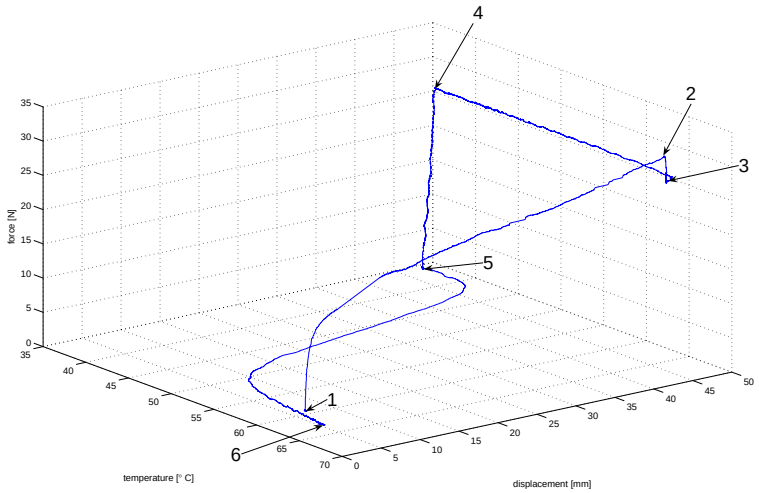

Fig. 22. *Working cycle of the shape memory polymer.*

4.2 Results

Veriflex® working cycle with 100% elongation is demonstrated in fig. 23 to 25 with different axes. It can be seen that for higher values of elongation, the real deformation has different value than the deformation computed from the specimen elongation. Relation between displacement Δl and deformation ε is defined by (2). l_0 is length of specimen with no deformation.

$$\varepsilon = \frac{\Delta l}{l_0} \tag{2}$$

Relation between real deformation ε_r and deformation ε is defined by (3).

$$\varepsilon_r = \ln(1+\varepsilon) \tag{3}$$

Relation between real stress σ_r and stress σ is defined by (4).

$$\sigma_r = \sigma \cdot (1+\varepsilon) \tag{4}$$

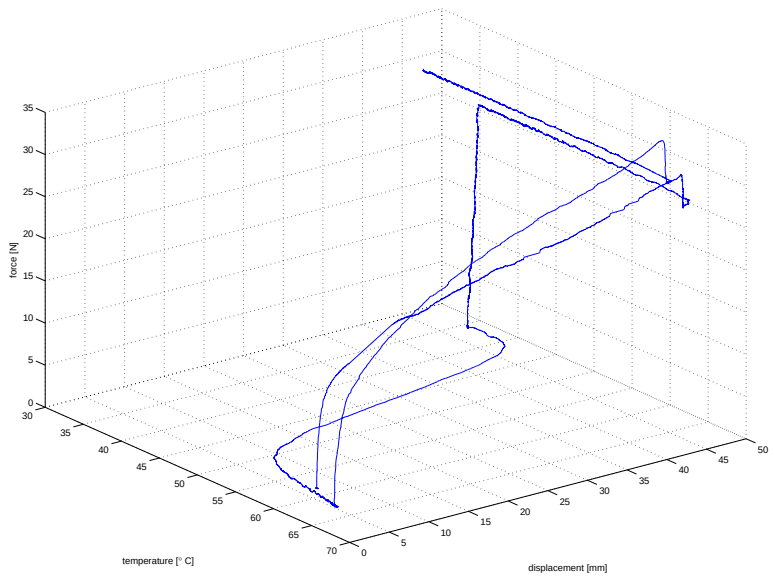

Fig. 23. *Veriflex® working cycle in displacement, temperature and force coordinates.*

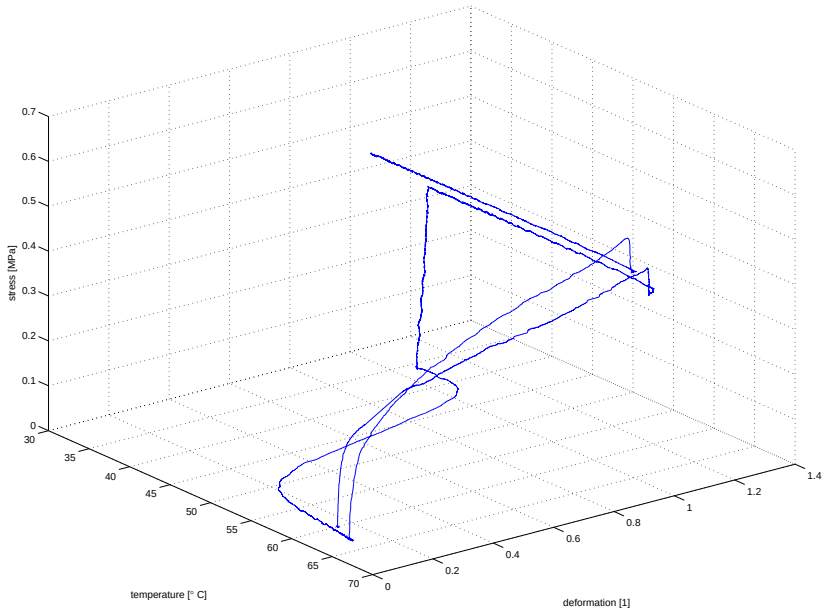

Fig. 24. *Veriflex® working cycle in deformation, temperature and stress coordinates.*

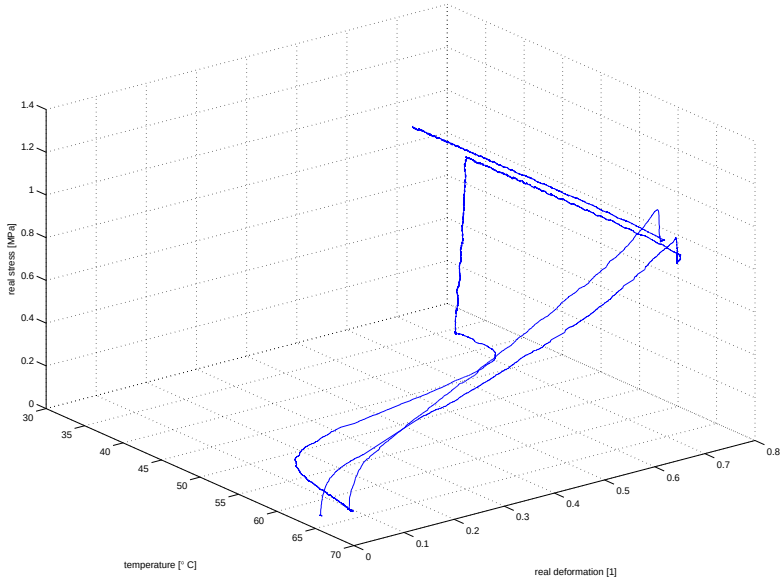

Fig. 25. *Veriflex® working cycle in real deformation, temperature and real stress coordinates.*

5. Conclusion

Experimental evaluation of properties of Veriflex® shape memory polymer was presented. It can be seen huge change of young modulus with temperature - from about 1000 MPa at 25° C to 1 MPa at 90° C. The results of tensile tests were shown and the working cycle of Veriflex® shape memory polymer was experimentally simulated. All these properties were studied for the purpose of future practical use in engineering applications.

Acknowledgements

This research was done in collaboration with the Department of Applied Mechanics of the University of Franche-Comté.

Nomenclature

a	horizontal shift factor	[1]
C_1	WLF theory universal constant	[1]
C_2	WLF theory universal constant	[K]
E'	storage modulus	[MPa]
E''	loss modulus	[MPa]
f	frequency	[Hz]
t	temperature	[º C]
t_g	glass transition temperature	[º C]
T	temperature	[K]
T_g	glass transition temperature	[K]
T_{ref}	reference temperature	[K]
δ	$\tan\delta = \frac{E'}{E''}$	[1]
ε	deformation	[1]
σ	stress	[MPa]
σ_{max}	tensile strength	[MPa]

References

[1] Henry, C. P., McKnight, G. P., Enke, A., Bortolin, R., Joschi, S., 3D FEA Simulation of Segmented Reinforcement Variable Stiffness Composites, Proceedings of SPIE Vol. 6929, 2008

[2] Dietsch, B., Tong, T., A Review – Features and Benefits of Shape Memory Polymers (SMPs), Journal of Advanced Materials, Vol. 39, No. 2, April 2007, pp 3-12

[3] Yakacki, C. M., Willis, S., Luders, C., Gall, K., Deformation Limits in Shape-Memory Polymers, Advanced Engineering Materials, Vol. 10, 2008, No. 1–2, pp 112-119

[4] Hayashi, S., Tasaka, Y., Hayashi, N., Akita, Y., Development of Smart Polymer Materials and its Various Applications, Mitsubishi Heavy Industries Ltd., Technical Review, Vol. 41, No. 1, February 2004

[5] Leng, J. S. et al., Electrical conductivity of thermoresponsive shape-memory polymer with embedded micron sized Ni powder chains, Applied Physics Letters 92, 014104, 2008

[6] Leng, J., Lv, H., Liu, Y., Du, S., Electroactivate shape-memory polymer filled with nanocarbon particles and short carbon fibers, Applied Physics Letters 91, 144105, 2007

[7] Coutu, D., Brailovski, V., Terriault, P., Fischer, C., Experimental validation of the 3D numerical model for an adaptive laminar wing with flexible extrados, 18th International Conference of Adaptive Structures and Technologies, October 3rd – 5th 2007, Ottawa, Ontario, Canada

[8] Liang, C., Rogers, C. A., Malafeew, E., Investigation of Shape Memory Polymers and Their Hybrid Composites, Journal of Intelligent Material Systems and Structures, Vol. 8, April 1997, pp 380-386

[9] Ohki, T., Ni, Q., Ohsako, N., Iwamoto, M., Mechanical and shape memory behavior of composites with shape memory polymer, Composites : Part A, Vol. 35, 2004, pp 1065-1073

[10] Keihl, M. M., Bortolin, R. S., Sanders, B., Joshi, S., Tidwell, Z., Mechanical Properties of Shape Memory Polymers for Morphing Aircraft Applications, Proceedings of SPIE Vol. 5762, 2005, pp 143-151
[11] Thill, C. et al., Morphing skins, The Aeronautical Journal, March 2008
[12] Bellin, I., Kelch, S., Langer, R., Lendleim, A., Polymeric triple-shape materials, Proceedings of the National Academy of Sciences, Vol. 103, 2006, No. 48, pp 18043-18047
[13] Ranta, D., Karger-Kocsis, J., Recent advances in shape memory polymers and composites: a review, Journal of Materials Science, Vol. 43, 2008, pp 254-269
[14] Liu, Y., Lv, H., Lan, X., Leng, J., Du, S., Review of electro-activate shape-memory polymer composite, Composites Science and Technology (2008), doi: 10.1016/ j.compscitech.2008.08.016
[15] Ledheim, A., Schmidt, A. M., Schroeter, M., Langer, R., Shape-Memory Polymer Networks from Oligo(ε-caprolactone)Dimethacrylates, Journal of Polymer Science: Part A: Polymer Chemistry, Vol. 43, 2005, pp 1369–1381
[16] Lendlein, A., Kelch, S., Shape-Memory Polymers, Angewandte Chemie Int. Ed., Vol. 41, 2002, pp 2034-2057
[17] Behl, M., Lendlein, A., Shape-memory polymers, Materials Today, Vol. 10, No. 4, April 2007, pp 20-28
[18] Nelson, B. A., King, W. P., Gall, K., Shape recovery of nanoscale imprints in a thermoset "shape memory" polymer, Applied Physics Letters 86, 103108, 2005
[19] Leng, J. S. et al., Significantly reducing electrical resistivity by forming conductive Ni chains in a polyurethane shape-memory polymer/carbon-black composite, Applied Physics Letters 92, 204101, 2008
[20] Cao, Q., Chen, S., Hu, J., Liu, P., Study on the Liquefied-MDI-Based Shape Memory Polyurethanes, Journal of Applied Polymer Science, Vol. 106, 2007, pp 993-1000
[21] Rauscher, S. G., Testing and Analysis of Shape-memory Polymers for Morphing Aircraft Skin Application, thesis, University of Pittsburg, 2008
[22] Gall, K. et al., Thermomechanics of the shape memory effect in polymers for biomedical applications, published online 1 April 2005 in Wiley InterScience (www.interscience.wiley.com), DOI: 10.1002/jbm.a.30296
[23] Jones, N. et al., Towards self-disassembling vehicles, The Journal of Sustainable Product Design, Vol. 3 , 2003, pp 59-74
[24] Chen, S., Hu, J., Zhuo, H., Zhu, Y., Two-way shape memory effect in polymer laminates, Materials Letters, Vol. 62, 2008, pp 4088-4090
[25] Yakacki, C. M. et al., Unconstrained recovery characterization of shape-memory polymer networks for cardiovascular applications, Biomaterials, Vol. 28, 2007, pp 2255-2263
[26] McKnight, G., Henry, C., Variable Stiffness Materials for Reconfigurable Surface Applications, Proceedings of SPIE Vol. 5761, 2005, pp 119-126
[27] Huang, W. M., Yang, B., An, L., Li, C., Chan, Y. S., Water-driven programmable polyurethane shape memory polymer: Demonstration and mechanism, Applied Physics Letters 86, 114105, 2005
[28] Leng, J., Lv, H., Liu, Y., Du, S., Comment on “Water-driven programmable polyurethane shape memory polymer: Demonstration and mechanism” [Appl. Phys. Lett. 86, 114105 (2005)], Applied Physics Letters 92, 206105, 2008
[29] Schmidt, C., Neuking, K., Eggeler, G., Functional Fatigue of Shape Memory Polymers, Advanced Engineering Materials, vol. 10, 2008, No. 10, pp 922 - 927